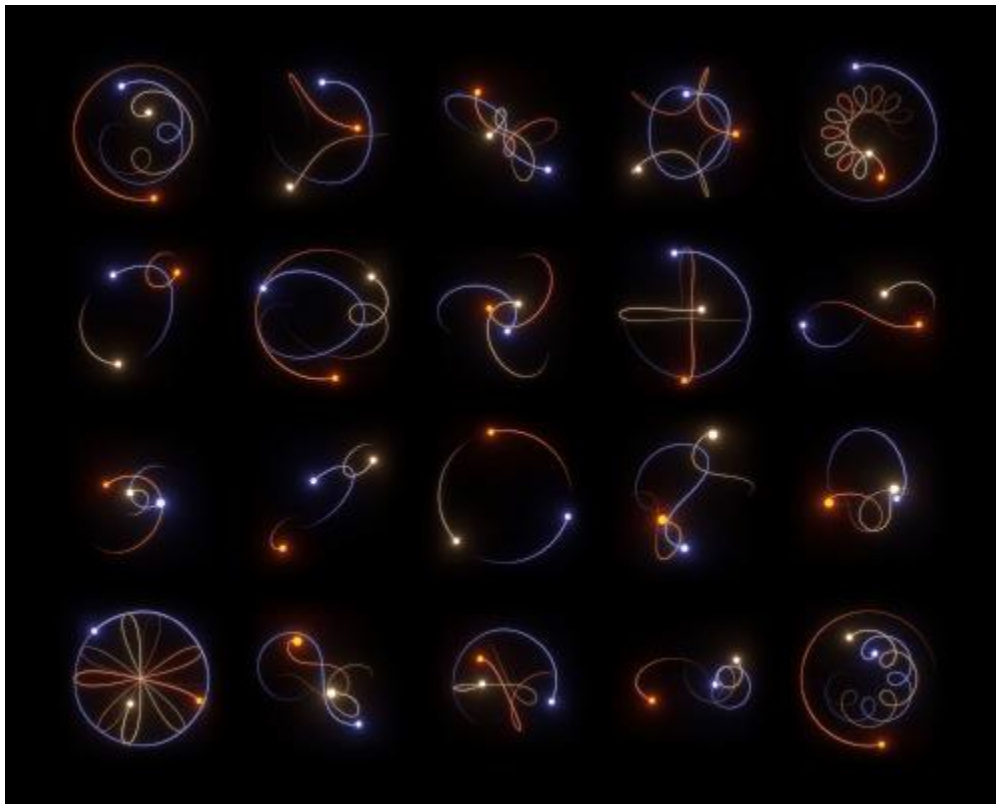


The Three Body Problem - Lagrange Points

Aaron Dunne, Jack Higgins, Jack Murphy

Department of Theoretical Physics,

National University of Ireland, Maynooth, Ireland



Abstract

In this project we model the orbit of a satellite around the L4 Lagrange point of the Earth-Moon system. The behavior of the satellite is derived from Hamilton's equations of motion, and is examined under a variety of different initial conditions

Table of Contents

Table of Contents	1
Background	2
Introduction	3
Part 1: Deriving the Equations of Motion	5
Part 2: The Driving Function	6
Part 3: Error Analysis	9
Part 4: Further Orbit Testing	19
Acknowledgements and Conclusion	22
Python Script	24

Background

The 3-body problem (recently brought into public view by the 2024 Netflix series of the same name) is a famous classical mechanics problem of 3 point masses. Given initial positions and momenta for these point masses, their resulting trajectories can be calculated using Newton's Laws of Motion and Newton's Universal Gravitational Law.

Unlike 2-body problems, the 3-body problem has no general closed form solution. However, famed mathematician Joseph Luis Lagrange formulated what is now known as the Lagrangian method. He found that when one of these masses was trivial compared to the other two, such as a satellite orbiting 2 planetary bodies for instance, the system had several stationary points, two of which are stable.

These stationary points are known as Lagrange points L_1, \dots, L_5 (see Figure 1 below).

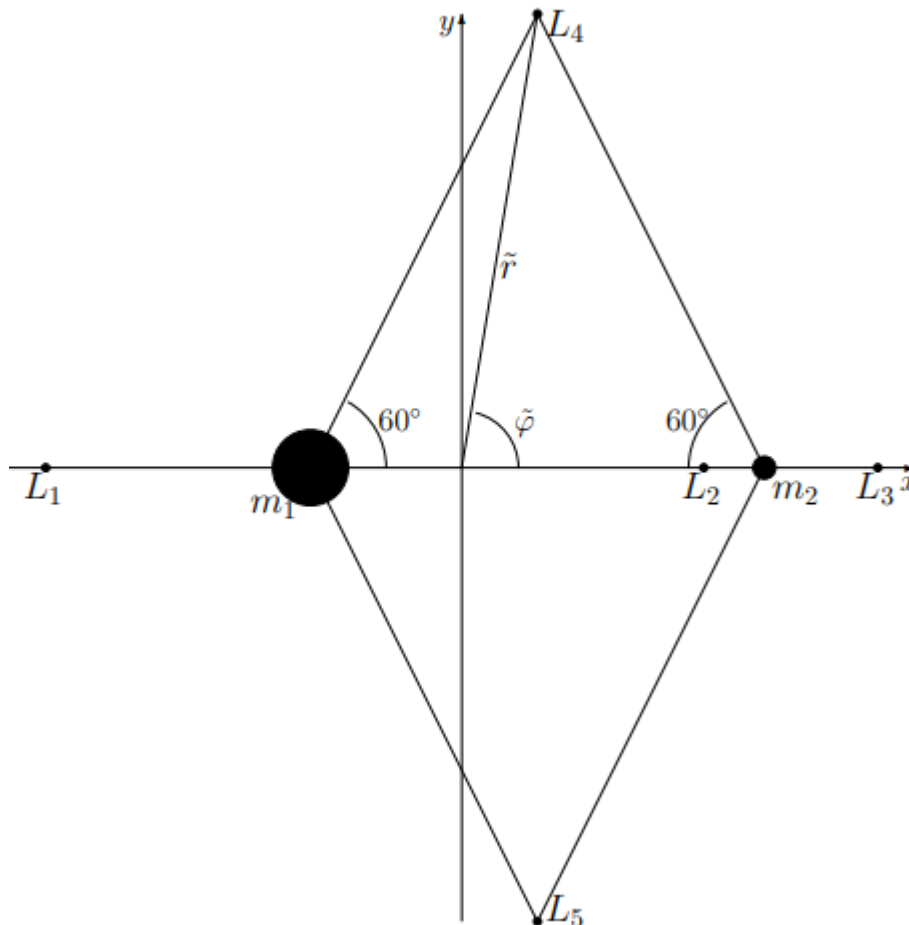


Figure 1: Lagrange Points of the system as defined in the introduction

Introduction

Consider a satellite of mass m' placed into orbit around the center of mass of the Earth-Moon system. This satellite's movement will be determined by its radial and angular momentum, alongside the force of gravity pulling on it from the earth and the moon (other planetary masses are negligible in this frame). In this project, we will aim to create a script that can trace the satellite's orbit over given periods of time in this system and produce graphs to display the orbit. We also intend to model the behaviour of satellite's placed near L4 and/or with varying initial momenta

To construct this, we first need to think about what kind of co-ordinate system we would like to use. For convenience, using the fact that the Earth and Moon rotate along their combined center of mass with constant angular velocity ω , we will choose a co-ordinate system fixed at this center of mass, and rotating at angular velocity ω . In this co-rotating frame, a satellite placed at (r, φ) will have kinetic energy;

$$T = \frac{m'}{2} \left[\left(\frac{dr}{dt} \right)^2 + r^2 \left(\frac{d\varphi}{dt} + \omega \right)^2 \right]$$

And will have potential energy;

$$V = -\frac{\gamma m_1 m'}{s_1} - \frac{\gamma m_2 m'}{s_2}$$

(See the end of this section for values of constants)

Using the potential and kinetic energy, we can construct the Lagrangian and hence, the Hamiltonian of this system. The reason for using Hamilton's equations instead of the Euler-Lagrange equations is that Hamilton's equations are first order O.D.E.s, whereas the Euler-Lagrange equations are second order O.D.E.s. Hamilton's equations are therefore simpler to solve computationally, and so more appropriate for this project.

The Lagrangian is given by;

$$L = T - V$$

Now, the Hamiltonian is given by;

$$H = \sum p_k \frac{dq_k}{dt} - L = \frac{p_r^2}{2m'} + \frac{p_\varphi^2}{2m' r^2} - p_\varphi \omega - \frac{\gamma m_1 m'}{s_1} - \frac{\gamma m_2 m'}{s_2}$$

(A full derivation of this can be seen later in figure 14)

Rescaling our co-ordinate system into more appropriately sized units, we define:

$$\tau \equiv \omega t \quad \tilde{r} \equiv \frac{r}{D} \quad \tilde{\varphi} \equiv \varphi \quad \tilde{p}_r \equiv \frac{p_r}{D\omega} \quad \tilde{p}_\varphi \equiv \frac{p_\varphi}{D^2\omega} \quad A_1 \equiv \frac{\gamma m_1}{D^3\omega^2} \quad A_2 \equiv \frac{\gamma m_2}{D^3\omega^2}$$

This gives the rescaled Hamiltonian;

$$\tilde{H} = \frac{H}{\omega^2 D^2} = \frac{\tilde{p}_r^2}{2m'} + \frac{\tilde{p}_\varphi^2}{2m'\tilde{r}^2} - \tilde{p}_\varphi - \frac{A_1 m'}{\tilde{s}_1} - \frac{A_2 m'}{\tilde{s}_2}$$

Values of Constants

$\omega = \frac{2\pi}{T}$ (where T is the period of rotation of the Earth and Moon about the center of mass of the system)

$D = 384,000$ km (Distance from the Earth to the Moon)

$\gamma = 6.674 \times 10^{-11} \frac{Nm^2}{kg^2}$ (Gravitational constant)

$m' = 1$ kg (Mass of satellite, trivial so set to 1 for ease of calculation)

$m_1 = 6 \times 10^{24}$ kg (Mass of the Earth)

$m_2 = 7 \times 10^{22}$ kg (Mass of the Moon)

$r_1 = D \frac{m_2}{m_1+m_2}$ (Radial position of Earth relative to center of mass)

$r_2 = D \frac{m_1}{m_1+m_2}$ (Radial position of the Moon relative to center of mass)

$\varphi_1 = \pi$ radians (Angular position of the Earth relative to center of mass)

$\varphi_2 = 0$ radians (Angular position of the Moon relative to center of mass)

$s_1 = \sqrt{r^2 + r_1^2 - 2rr_1 \cos(\varphi - \varphi_1)}$ (Distance from the satellite to Earth)

$s_2 = \sqrt{r^2 + r_2^2 - 2rr_2 \cos(\varphi - \varphi_2)}$ (Distance from the satellite to the Moon)

$\tilde{s}_1 = \sqrt{\tilde{r}^2 + \tilde{r}_1^2 - 2\tilde{r}\tilde{r}_1 \cos(\tilde{\varphi} - \tilde{\varphi}_1)}$ (Rescaled distance from the satellite to Earth)

$\tilde{s}_2 = \sqrt{\tilde{r}^2 + \tilde{r}_2^2 - 2\tilde{r}\tilde{r}_2 \cos(\tilde{\varphi} - \tilde{\varphi}_2)}$ (Rescaled distance from the satellite to the Moon)

Part 1: Deriving the Equations of Motion

Hamilton's Equations of Motion can be derived from the rescaled Hamiltonian as below;

$$\frac{d\tilde{q}_k}{d\tau} = \frac{\partial \tilde{H}}{\partial \tilde{p}_k}$$

$$\frac{d\tilde{p}_k}{d\tau} = -\frac{\partial \tilde{H}}{\partial \tilde{q}_k}$$

This gives;

$$\frac{d\tilde{r}}{d\tau} = \frac{\partial \tilde{H}}{\partial \tilde{p}_r} = \frac{\tilde{p}_r}{m'}$$

$$\frac{d\tilde{\varphi}}{d\tau} = \frac{\partial \tilde{H}}{\partial \tilde{p}_\varphi} = \frac{\tilde{p}_\varphi}{m' \tilde{r}^2} - 1$$

$$\frac{d\tilde{p}_r}{d\tau} = -\frac{\partial \tilde{H}}{\partial \tilde{r}} = \frac{\tilde{p}_\varphi^2}{m' \tilde{r}^3} - \frac{A_1 m'}{\tilde{s}_1^3} (\tilde{r} - \tilde{r}_1 \cos(\tilde{\varphi} - \tilde{\varphi}_1)) - \frac{A_2 m'}{\tilde{s}_2^3} (\tilde{r} - \tilde{r}_2 \cos(\tilde{\varphi} - \tilde{\varphi}_2))$$

$$\frac{d\tilde{p}_\varphi}{d\tau} = -\frac{\partial \tilde{H}}{\partial \tilde{\varphi}} = -\frac{A_1 m'}{\tilde{s}_1^3} (\tilde{r} \tilde{r}_1 \sin(\tilde{\varphi} - \tilde{\varphi}_1)) - \frac{A_2 m'}{\tilde{s}_2^3} (\tilde{r} \tilde{r}_2 \sin(\tilde{\varphi} - \tilde{\varphi}_2))$$

These equations were then verified by evaluating the derivatives at L_4 which is given by

$$\tilde{r}_{L_4} = \sqrt{\tilde{r}_1^2 - \tilde{r}_1 + 1}$$

$$\tilde{\varphi}_{L_4} = \cos^{-1} \left(\frac{2\tilde{r}_2 - 1}{2\tilde{r}_{L_4}} \right)$$

$$\tilde{p}_{r_{L_4}} = 0$$

$$\tilde{p}_{\varphi_{L_4}} = \tilde{r}_{L_4}^2 m'$$

This was done computationally and returned an array of zeros, as expected of a stationary point such as L_4

(**Note:** The $\frac{d\tilde{p}_k}{d\tau}$ terms returned values of order $\pm 10^{-18}$ which is within machine precision of zero and thus was taken to be zero)

Part 2: The Driving Function

After vectorizing the derivatives calculated in Part 1, we used odeint to construct a matrix whose columns were arrays of $\tilde{r}(\tau)$, $\tilde{p}_r(\tau)$, $\tilde{\varphi}(\tau)$ and $\tilde{p}_\varphi(\tau)$ respectively. We then extracted these arrays and converted them to Cartesian co-ordinates using the equations;

$$x = \tilde{r} \cos(\tilde{\varphi})$$

$$y = \tilde{r} \sin(\tilde{\varphi})$$

We then tested the following set of initial conditions and plotted the results for various lengths of time with (0,0) being the center of mass of the system (see Figures 2-5 below);

$$r_0 = 1.001 \times \tilde{r}_{L_4}$$

$$\varphi_0 = \tilde{\varphi}_{L_4}$$

$$p_{r_0} = 0.001$$

$$p_{\varphi_0} = r_0^2 m'$$

Note:

For each of the graphs in Figures 2 - 5

-1 unit of length is 384,000km, about the average distance from the earth to the moon

-To track an orbit over roughly 1 month, we would input $\tau=6$

i.e. - τ corresponds to about 5 days

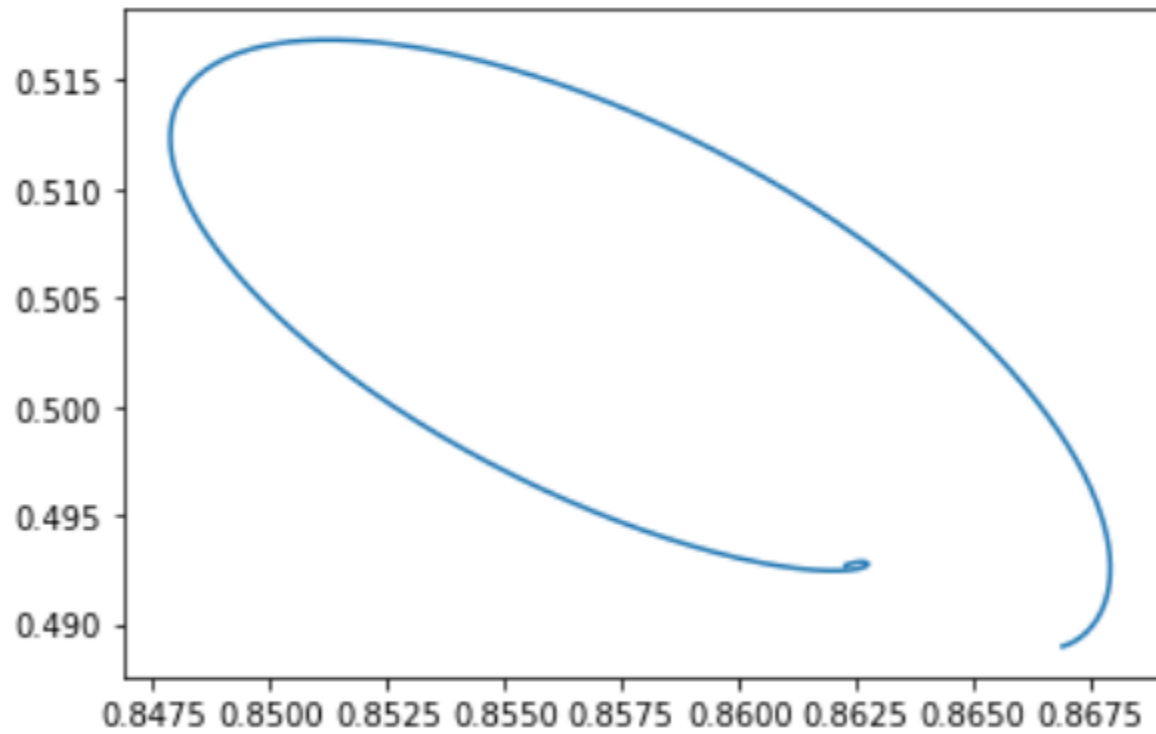


Figure 2: Orbit after 10τ - about 6 weeks

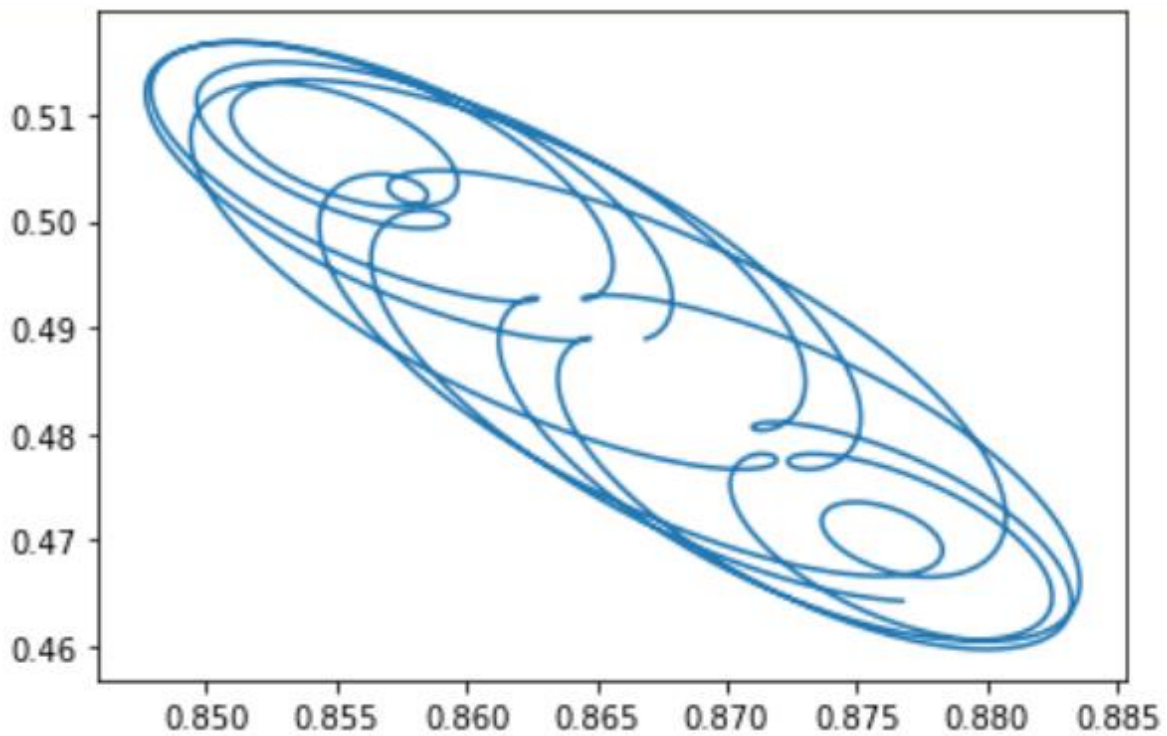


Figure 3: Orbit after 100τ - about 16 months, elliptical pattern becoming distinguishable

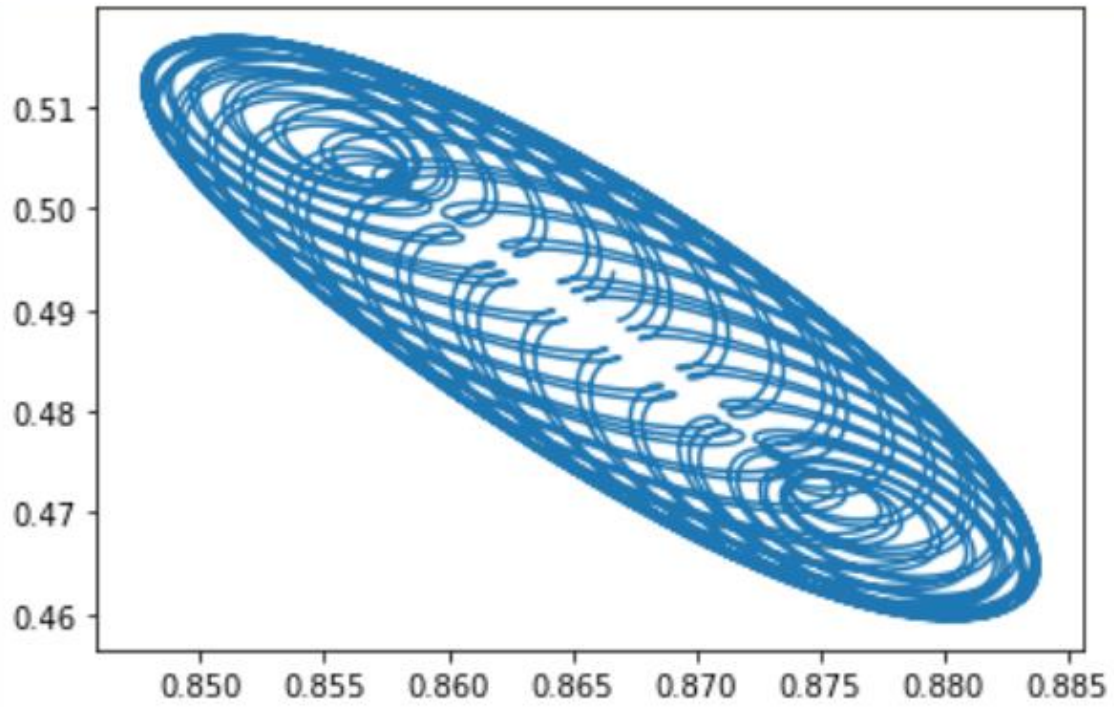
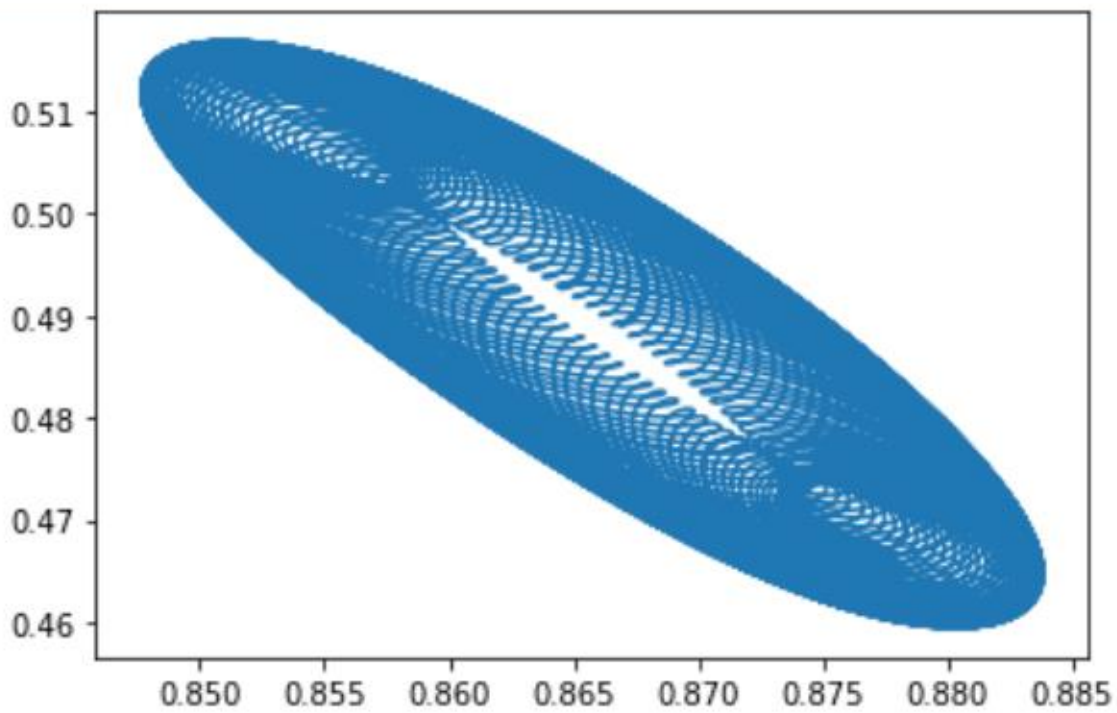


Figure 4: Orbit after 500τ about 7 years, elliptical pattern begins overlapping with itself



5: Orbit after 1000τ - about 13 years, elliptical pattern clearly visible

Figure

Part 3: Error Analysis

In the first version of our code there were two notable errors in our derivative function;

The $\frac{d\tilde{p}_r}{d\tau}$ and $\frac{d\tilde{p}_\phi}{d\tau}$ terms were both non-zero when evaluated at L_4 which resulted in the satellite erratically bouncing around (see Figures 6-8 below).

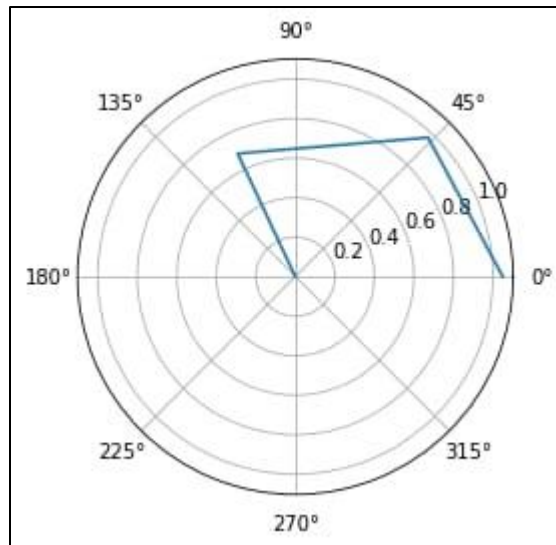


Figure 6: Satellite bouncing after 10τ

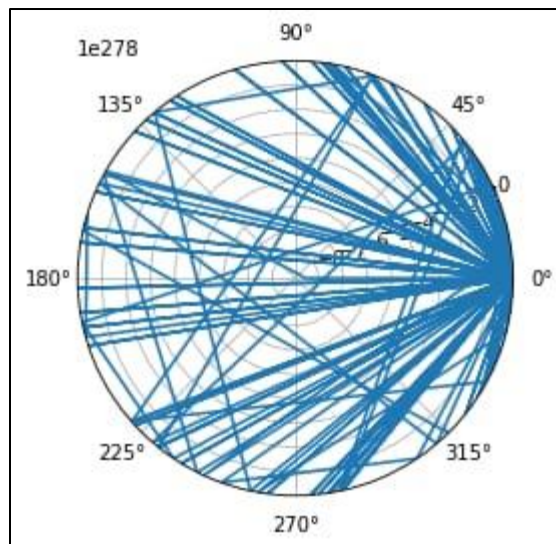


Figure 7: Satellite bouncing after 100τ

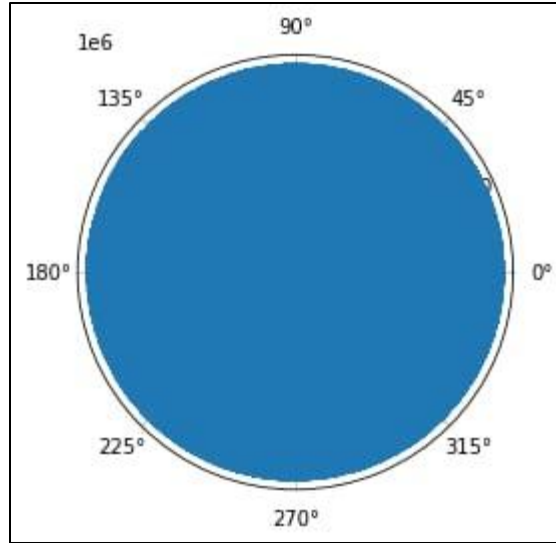


Figure 8: Satellite bouncing after 1000τ

Plotting each component in Cartesian co-ordinates highlights the error more clearly as each of these terms should be constant at L_4 (see Figure 9 below).

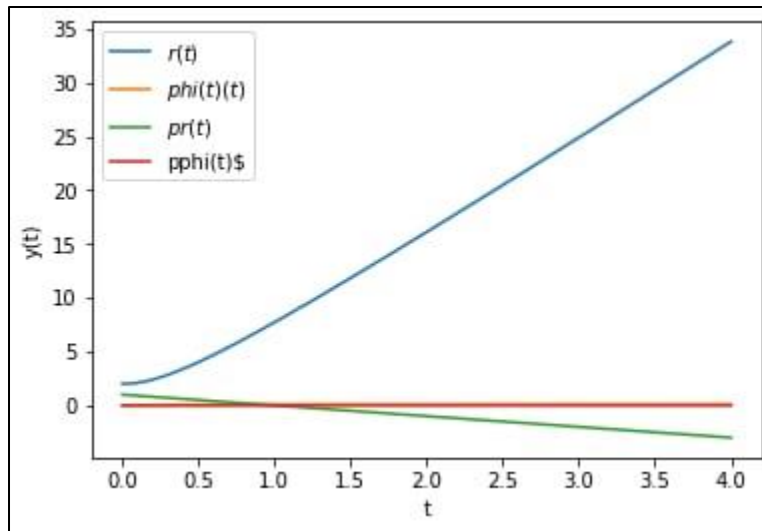


Figure 9: Erroneous values

The error in the $\frac{d\tilde{p}_\phi}{d\tau}$ term was caused by an error in our initial calculations and was corrected by re-deriving the equations of motion. The error in the $\frac{d\tilde{p}_r}{d\tau}$ term proved to be significantly more challenging to correct.

After re-deriving the equations of motion several times, evaluation at L_4 was resulting in $\frac{d\tilde{p}_r}{d\tau} \approx -9.8 \times 10^{-1}$ which is clearly non-zero and well within machine precision.

Additionally, this error was causing an overflow when testing with odeint, resulting in a satellite which would seemingly teleport to well outside the bounds of the observable universe before teleporting back to the center of mass of the system (see Figure 10 Below).

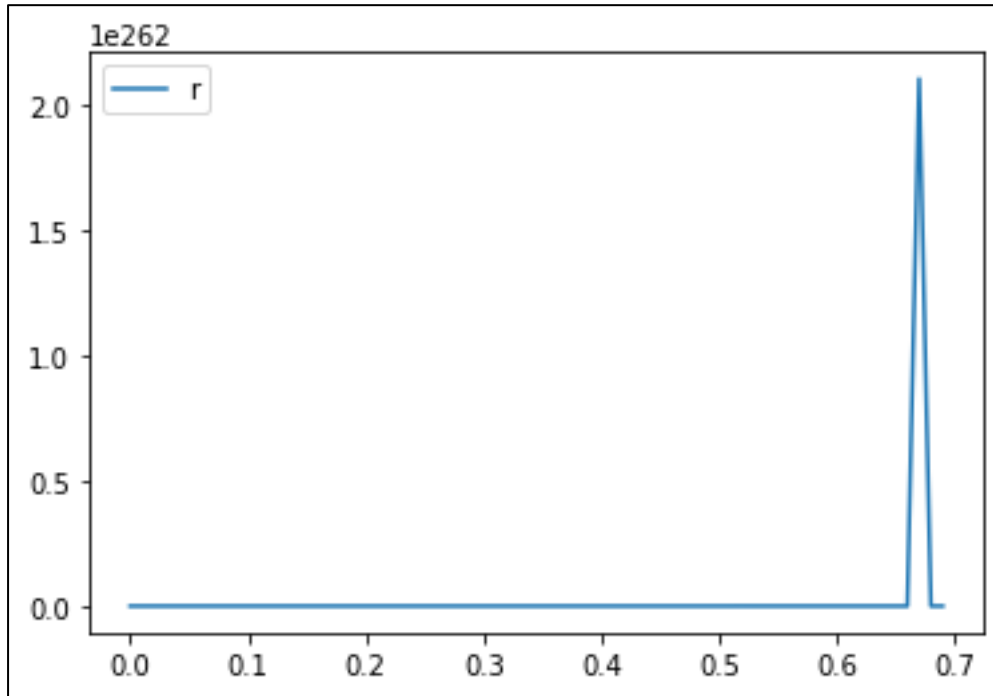


Figure 10: The satellite supposedly jumping to $D \times 10^{262}\text{km}$

This error was also causing parts of the graph of $\tilde{p}_\phi(\tau)$ to be discontinuous in addition to having an overflow error (see Figure 10 Below).

Plotting these against each other resulted in several aesthetically interesting graphs (see Figures 11 and 12 below). However, most notably, these graphs were different each time the code was run.

Converting to Cartesian co-ordinates resulted in a satellite which drifted endlessly through space (see Figure 13 below).

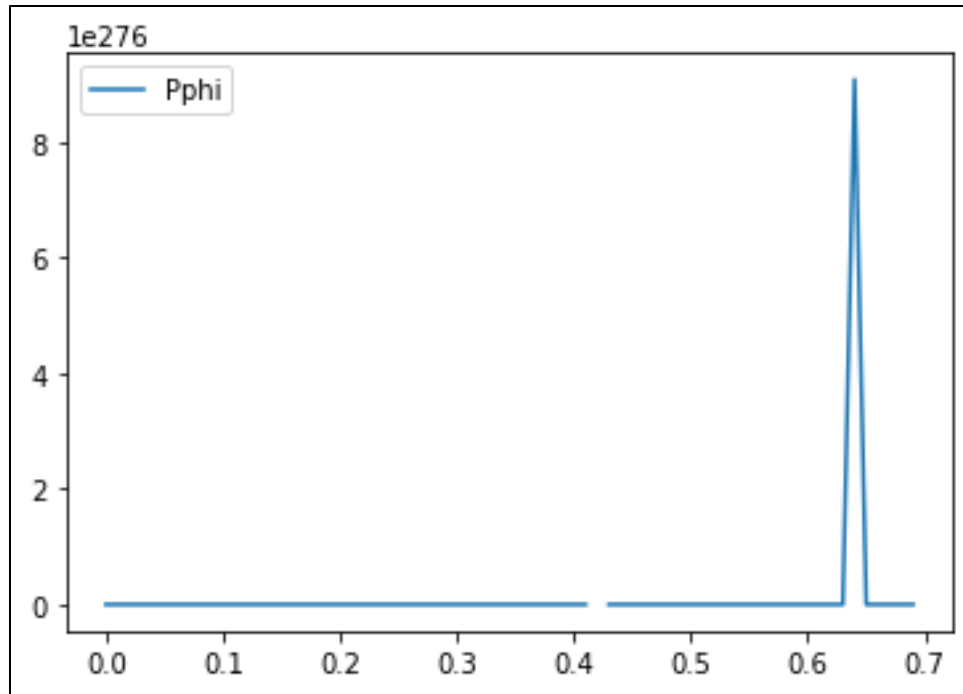


Figure 10: $\tilde{p}_\varphi(\tau)$ is both discontinuous and overflowing

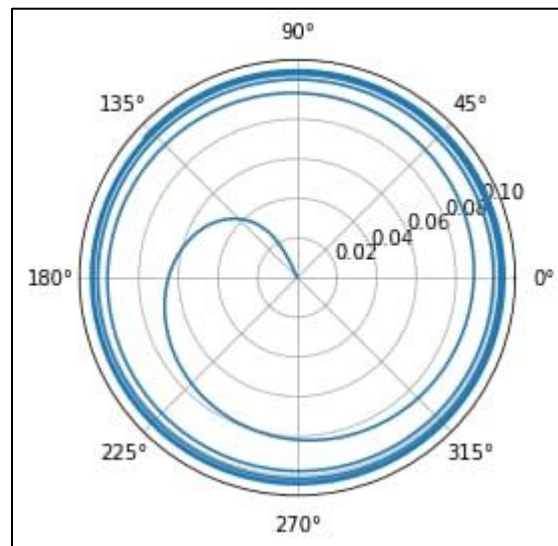


Figure 11: The satellite appears to orbit the center of mass in one iteration

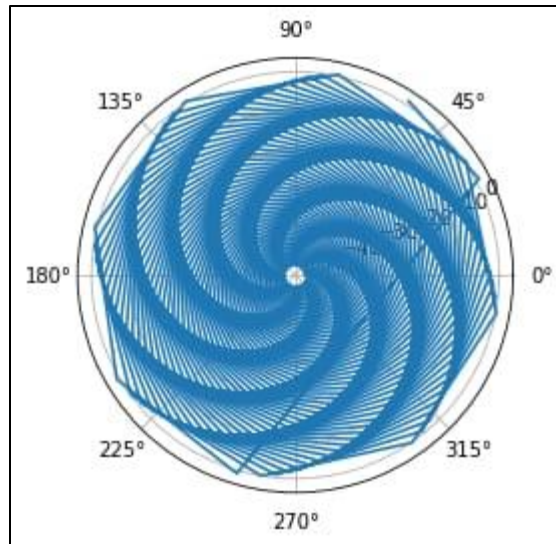


Figure 12: The satellite appears to bounce around in a rather beautiful yet meaningless spiral pattern in another iteration

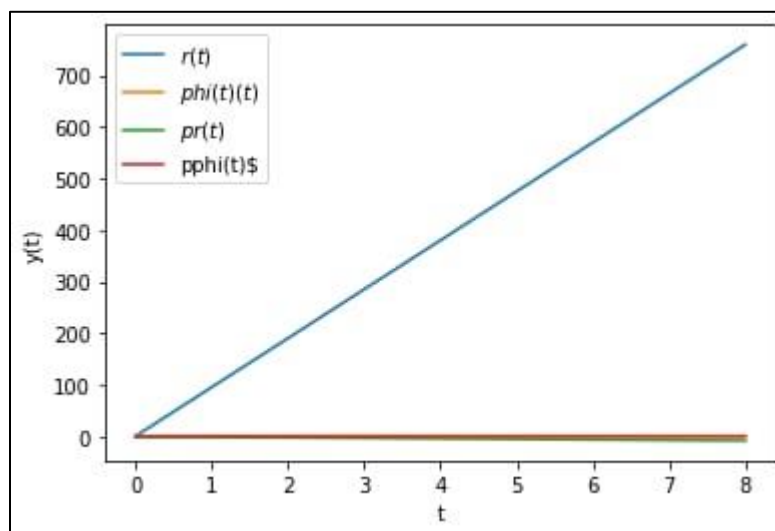


Figure 13: In Cartesian co-ordinates the satellite appears to drift endlessly

After re-deriving the equations of motion until we were satisfied we had not made any mistakes in our calculus we determined that we must have made an error in our implementation of the code.

After re-syntaxing and getting the same result, we tried altering our code in the following ways;

- Replacing integer exponents with decimals to ensure use of floating-point arithmetic
- Replacing negative exponents with quotients
- Algebraically simplifying the expressions where possible
- Altering the initial conditions
- Altering the value of μ (The original brief had $\mu \equiv \frac{m_2}{m_1}$)
- Altering $d\tau$ step size
- Manipulating the equation to avoid division by small numbers
- Substitution of variables
- Setting various variable equal to 1 to identify problem points
- Defining variables explicitly to reduce rounding error

At this point we believed that there might be specific values of τ that caused the equations to blow up to infinity. We used the graphs of each variable against τ to roughly identify the point at which it blows up. For example, in Figure 9 we can see that $\tilde{r}(\tau)$ blows up around 0.6-0.7.

We then set these values as bounds on τ and printed an array of the function's outputs at each step $d\tau$.

After all our attempts to find a bug in the code failed, we decided to investigate the expression for the Hamiltonian we were given in the brief, as well as the initial conditions.

We began our investigation by manually calculating the value of $\frac{d\tilde{p}_r}{d\tau}$ at L_4 given by our Hamilton equations and found that they gave the exact same answer that had been computed by our code up to a rounding error.

This led us to conclude that the error was not in our code, but somewhere in the brief itself, and so we knew that we had to fact-check the brief.

We began by re-deriving the unscaled Hamiltonian from scratch (see Figure 14 for derivation) and found that the unscaled Hamiltonian we were given was incorrect.

Brief Error 1: The Hamiltonian

Original Hamiltonian:

$$H = \frac{p_r^2}{2\mu} + \frac{p_\varphi^2}{2\mu r^2} - p_\varphi \omega - \frac{\gamma m_1 m'}{s_1} - \frac{\gamma m_2 m'}{s_2}$$

Correct Hamiltonian:

$$H = \frac{p_r^2}{2m'} + \frac{p_\phi^2}{2m'r^2} - p_\phi\omega - \frac{\gamma m_1 m'}{s_1} - \frac{\gamma m_2 m'}{s_2}$$

This erroneous Hamiltonian had μ in place of m' in the denominator of the first two terms and was otherwise correct. This error scaled the first two terms by a factor of $\frac{1}{\mu} \approx 86$ and did not scale the other terms. Consequently, we had been working on a Hamiltonian which described an entirely different system and therefore our Hamilton equations, although derived correctly, were not the equations of motion for our system.

Once we had corrected the unscaled Hamiltonian, we moved on to scaling it. In doing so, we found an error in the scaling of the variables.

Brief Error 2: Scaling

Original Scaling:

$$p_r = D\omega\tilde{p}_r$$

Correct Scaling:

$$p_r = \frac{\tilde{p}_r}{D\omega}$$

With the help of Jonivar and some dimensional analysis, we found a suitable scaling which satisfied the condition $H = D^2\omega^2\tilde{H}$, which was the scaling suggested in the brief. The original scaling had \tilde{p}_r multiplied by $D\omega$, whereas the correct scaling has \tilde{p}_r divided by $D\omega$ and so \tilde{p}_r had been incorrectly scaled by a factor of $(D\omega)^2 \approx 1.044$ with respect to the other variables.

Although this error is of a lower order than the last, it still meant that we had not been describing the correct system.

Now that we had the correct scaled Hamiltonian, we re-derived Hamilton's equations and obtained the equations of motions for this system. During this process, Jonivar brought it to our attention that the initial conditions we had been given were also incorrect.

Brief Error 3: Initial Conditions

Original Initial Conditions:

$$\begin{aligned}\tilde{r}_{L_4} &= \sqrt{\tilde{r}_1^2 - \tilde{r}_1 + 1} \\ \tilde{\varphi}_{L_4} &= \cos^{-1}\left(\frac{\tilde{r}_{L_4}^2 + \tilde{r}_2^2 - 1}{2\tilde{r}_{L_4}\tilde{r}_2}\right) \\ \tilde{p}_{r_{L_4}} &= 0 \\ \tilde{p}_{\varphi_{L_4}} &= \tilde{r}_{L_4}^2 \mu\end{aligned}$$

Correct initial conditions:

$$\begin{aligned}\tilde{r}_{L_4} &= \sqrt{r_1^2 - \tilde{r}_1 + 1} \\ \tilde{\varphi}_{L_4} &= \cos^{-1}\left(\frac{2\tilde{r}_2 - 1}{2\tilde{r}_{L_4}}\right) \\ \tilde{p}_{r_{L_4}} &= 0 \\ \tilde{p}_{\varphi_{L_4}} &= \tilde{r}_{L_4}^2 m'\end{aligned}$$

We were able to verify the original values of \tilde{r}_{L_4} and $\tilde{\varphi}_{L_4}$ by geometrically deriving them using the diagram in Figure 1 (see Figure 15 below for derivations). However, Jonivar found the correct $\tilde{p}_{\varphi_{L_4}}$ which like the original Hamiltonian, should have had m' in place of μ .

Once we had corrected the Hamiltonian, equations of motion and initial conditions, we were satisfied that there was nothing left that could have been wrong and so applied all of these corrections to our script. We modified the vectorized system of O.D.E.s accordingly and inputted the correct initial conditions and our script generated outputs describing a stable orbit, concluding our error analysis.

• The first step is to find the Lagrangian:

$$T = \frac{m'}{2} \dot{r}^2 + \frac{m'}{2} r^2 (\dot{\phi} + \omega)^2 \quad \text{where } \dot{r} = \frac{dr}{dt}, \dot{\phi} = \frac{d\phi}{dt}$$

$$V = -\frac{\gamma m_1 m'}{s_1} - \frac{\gamma m_2 m'}{s_2}$$

$$\text{So } L = \frac{m'}{2} \dot{r}^2 + \frac{m'}{2} r^2 (\dot{\phi} + \omega)^2 + \frac{\gamma m_1 m'}{s_1} + \frac{\gamma m_2 m'}{s_2}$$

• Next, we find the Hamiltonian, $H = (p_r)(\dot{r}) + (p_\phi)(\dot{\phi}) - L$

$$p_r = \frac{\partial L}{\partial \dot{r}} = m' \dot{r}, \quad p_\phi = \frac{\partial L}{\partial \dot{\phi}} = m' r^2 (\dot{\phi} + \omega)$$

$$\Rightarrow H = (m' \dot{r})(\dot{r}) + (m' r^2 (\dot{\phi} + \omega))(\dot{\phi}) - \left[\frac{m'}{2} \dot{r}^2 + \frac{m'}{2} r^2 (\dot{\phi} + \omega)^2 - \frac{\gamma m_1 m'}{s_1} - \frac{\gamma m_2 m'}{s_2} \right]$$

- Easier to break this sum into three parts:

* Radial term: $m' \dot{r}^2 - \frac{m'}{2} \dot{r}^2 = \frac{1}{2} m' \dot{r}^2 = \frac{(m' \dot{r})^2}{2m'} = \frac{p_r^2}{2m'}$

* Angular term: $(m' r^2)(\dot{\phi} + \omega)\dot{\phi} - \frac{m'}{2} r^2 (\dot{\phi} + \omega)^2$

$$= m' r^2 \dot{\phi}^2 + m' r^2 \dot{\phi} \omega - \frac{m'}{2} r^2 \dot{\phi}^2 - m' r^2 \dot{\phi} \omega - \frac{m'}{2} r^2 \omega^2$$

$$= \frac{1}{2} m' r^2 \dot{\phi}^2 + m' r^2 \dot{\phi} \omega - \frac{m'}{2} r^2 \omega^2 - m' r^2 \dot{\phi} \omega - m' r^2 \omega^2$$

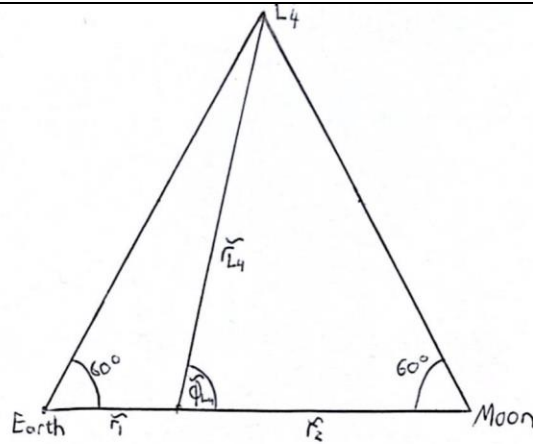
$$= \frac{1}{2m' r^2} ((m')^2 r^4 \dot{\phi}^2 + 2(m')^2 r^4 \dot{\phi} \omega + (m')^2 r^4 \omega^2) - \omega(m' r^2 \dot{\phi} + m' r^2 \omega)$$

$$= \frac{1}{2m' r^2} (m' r^2 \dot{\phi} + m' r^2 \omega)^2 - \omega(m' r^2 \dot{\phi} + m' r^2 \omega) = \frac{p_\phi^2}{2m' r^2} - p_\phi \omega$$

* Potential term: $-\frac{\gamma m_1 m'}{s_1} - \frac{\gamma m_2 m'}{s_2}$

Subbing back in: $H = \frac{p_r^2}{2m'} + \frac{p_\phi^2}{2m' r^2} - p_\phi \omega - \frac{\gamma m_1 m'}{s_1} - \frac{\gamma m_2 m'}{s_2}$

Figure 14: Unscaled Hamiltonian derivation



- This triangle is equilateral, so all sides have a length equal to the Earth-Moon distance, which is 1 in the new scaled co-ordinate system.

- Therefore, we can use the cosine rule to get

$$\begin{aligned}\tilde{r}_{L_4} &= \sqrt{\tilde{r}_1^2 + (1)^2 - 2\tilde{r}_1(1)\cos(60^\circ)} \\ &= \sqrt{\tilde{r}_1^2 - \tilde{r}_1 + 1}\end{aligned}$$

$$(\text{or alternatively } \tilde{r}_{L_4} = \sqrt{\tilde{r}_2^2 - \tilde{r}_2 + 1})$$

- We can also use the cosine rule to find $\tilde{\phi}_{L_4}$

$$(1)^2 = \tilde{r}_{L_4}^2 + \tilde{r}_2^2 - 2\tilde{r}_{L_4}\tilde{r}_2\cos(\tilde{\phi}_{L_4})$$

$$\Rightarrow \tilde{\phi}_{L_4} = \cos^{-1}\left(\frac{\tilde{r}_{L_4}^2 + \tilde{r}_2^2 - 1}{2\tilde{r}_{L_4}\tilde{r}_2}\right)$$

substituting $\tilde{r}_{L_4} = \sqrt{\tilde{r}_2^2 - \tilde{r}_2 + 1}$ we can simplify:

$$\tilde{\phi}_{L_4} = \cos^{-1}\left(\frac{\tilde{r}_2^2 - \tilde{r}_2 + 1 + \tilde{r}_2^2 - 1}{2\tilde{r}_{L_4}\tilde{r}_2}\right)$$

$$= \cos^{-1}\left(\frac{2\tilde{r}_2 - 1}{2\tilde{r}_{L_4}}\right)$$

Figure 15: \tilde{r}_{L_4} and $\tilde{\phi}_{L_4}$ derivations

Part 4: Further Orbit Testing

Limitations of our model

This model only considers the existence of the moon and the Earth and thus produces less and less accurate results the further the initial conditions deviate from L_4 .

Additionally, our model only allows for deviations from L_4 specifically and does not explore the behavior around any of the other Lagrange points.

Some other orbits

Several interesting orbits can be observed by varying the deviation of each initial condition from L_4

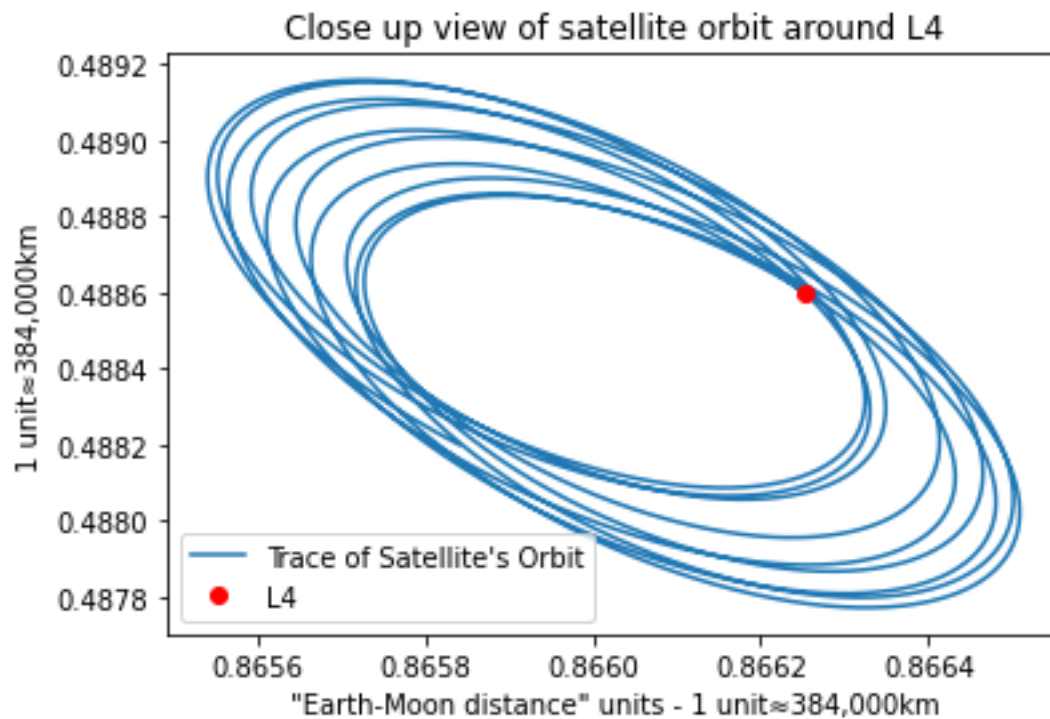


Figure 16: 100km radial deviation for 10 months

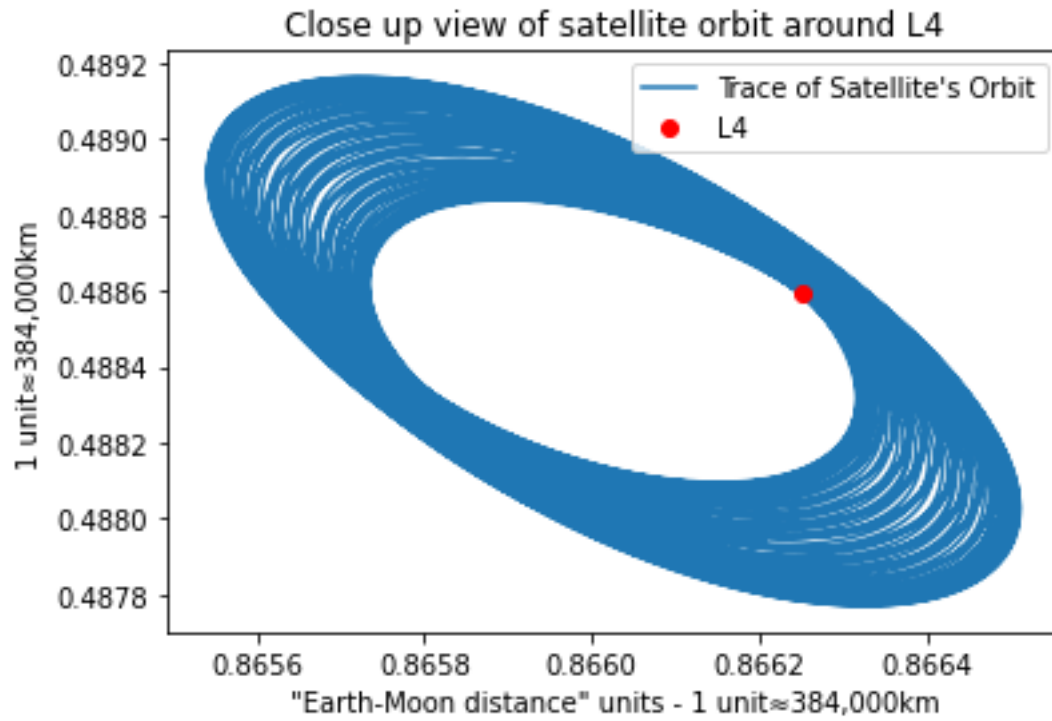


Figure 17: 100km radial deviation for 100 months

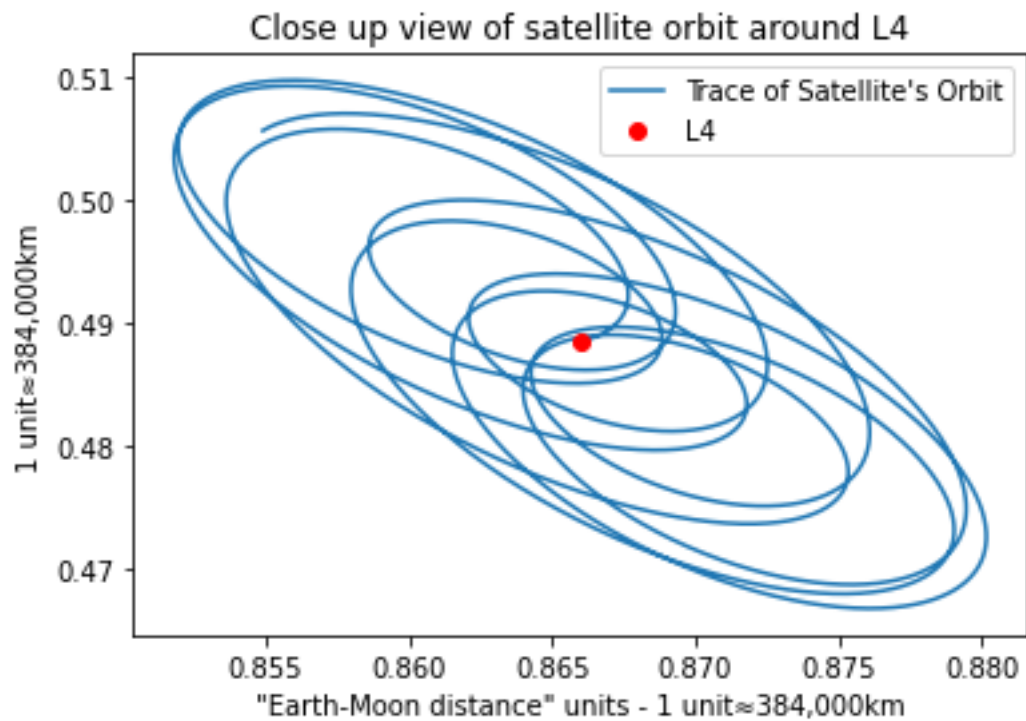


Figure 18: 0.005 momentum conjugate to radius deviation for 10 months

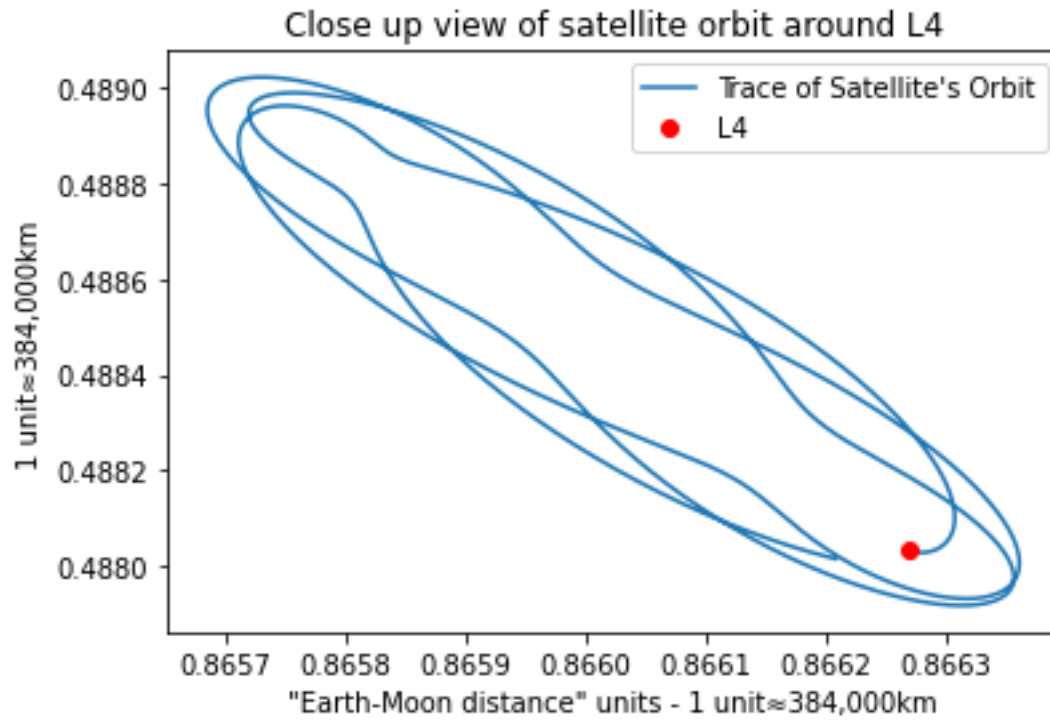


Figure 19: 0.0005 radian deviation of $\tilde{\varphi}$ for 10 months

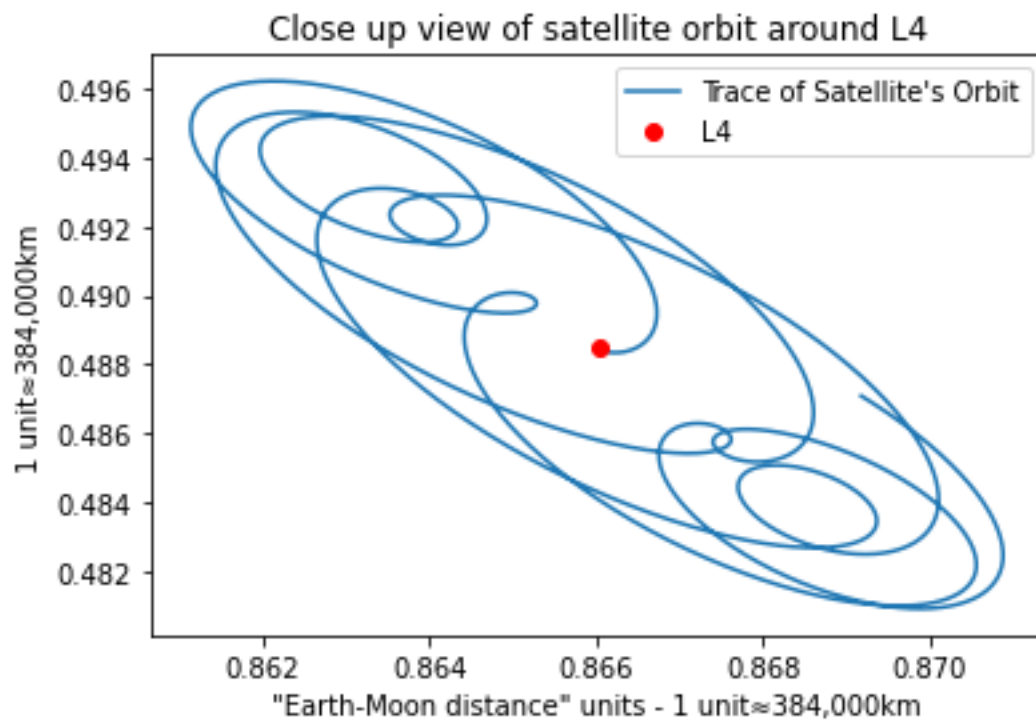


Figure 20: 0.0005 momentum conjugate to $\tilde{\varphi}$ deviation for 10 months

Further research possibilities

The orbits shown in Figures 16 - 20 Above are far from an exhaustive list of those possible.

One possible avenue for further research would be to try to construct some of the more famous orbits such as the “Horseshoe” or “Kidney” orbits. Additionally, experimenting with different combinations of deviations may produce many more interesting orbits.

Also, as mentioned in the beginning of Part 4, our model becomes less accurate the further the deviation from L_4 . Further study of where exactly the model begins to break down would be a useful starting point for developing more advanced models. Our model could also be expanded to consider the other Lagrange points within this system. A suitable place to start would be deriving the conditions for L_5 and allowing for deviations from it as well, before expanding the model to include the non-stable points L_1 , L_2 and L_3 and studying the behaviour of a satellite about these points.

Finally, the masses of each of the 2 larger bodies and the distance between them could also be varied to see what effect this would have on the types of orbits possible.

Acknowledgements and Conclusion

Conclusion

The three body problem is one that has fascinated physicists for centuries. The existence of Lagrange points was first discovered over 250 years ago at a time when there was no practical way to graph the movement of objects at these points through space. Fortunately for us, we have the opportunity to do so using the computational techniques we have amassed over the course of this project. We verified the stability of orbits around L_4 , demonstrating that an object placed exactly at L_4 with the correct momentum will remain stationary with respect to our frame. Through investigating the movement of objects near L_4 , we also discovered emergent patterns in their orbits over extended periods of time, that otherwise would have been significantly more difficult to understand.

Models like the one we have produced have been crucial in the development and maintenance of modern satellite communication, as well as extraterrestrial observational technologies.

Acknowledgements

We would like to thank Dr. Jonivar Skullerud as well as Mr. Dale Lawlor and Ms. Hannah O'Brennan whose support and guidance made this project possible.

Cover image sourced from Eya Minati's Medium article on the three-body problem

(<https://medium.com/@eyaminati/three-body-problem-in-physics-04a9ec4553fb>)